Paper No. 196

Performance evaluation of a filter-based pseudo-negative stiffness control for seismically isolated structures`

Wei Gong, Shishu Xiong
School of Civil Engineering and Mechanics, Huazhong University of Science and Technology, Wuhan 430074, Hubei, PR China

ABSTRACT

Research shown in this paper is focused on the development of a new filter-based pseudo-negative stiffness (FPNS) control algorithm, which aims to overcome the challenge of the sudden change of control force produced by the conventional PNS control force. The strategy of this method is to produce a negative stiffness friction damping force with a gradual change at velocity switches by employing a low-pass filter. By investigating the time-history curves and the hysteresis loops of the FPNS control force, it is found that the low-pass filter also enables the control force at the original position increases with increasing seismic intensities and helps roll off the high-frequency component of the control force. Only the relative displacement of control devices is required for measurement.

A semi-active design is developed to produce the desired reference control force by MR dampers. The structure used for numerical simulation is the base-isolated benchmark building. Seismic responses of the FPNS control, the simple displacement PNS control, the sample semi-active control and the optimal viscous damping control are compared under different seismic intensities. The effectiveness of each control case is evaluated based on the 'ideal isolation control principle'. The results show that the FPNS control can improve the isolation functionality for both low-to-moderate and extreme seismic intensities as well as enhance the isolation safety.

Keywords: *base isolation, pseudo-negative stiffness control, benchmark problem, semi-active control*

1 INTRODUCTION

Base isolation has been well accepted as a simple, reliable and effective technology to protect structures from earthquake hazard. The system by itself can reduce the absolute floor acceleration and the inter-story drift of the superstructure by introducing flexible isolation devices between the superstructure and the supporting foundation, but extensive deformation of isolation devices may be observed during extreme earthquakes, which has raised serious questions about the safety of base-isolated structures. A method to accommodate the large displacement is to add some passive damping at the isolation level to dissipate the seismic input energy. However, excessive damping required for base displacement reduction may cause significant force transmitted to the superstructure. Kelly [1] has pointed out that the passive dampers, although controlling displacements, drive energy into higher modes and defeat the primary reason for using isolation-namely, the reduction of inter-story drift and floor acceleration. An alternative to solve the dilemma is to incorporate the semi-active control system within the isolation system. Compared to passive dampers, the semi-active system offers a potential increase in damping efficiency. However, this strongly depends on the control algorithm employed.

Among a variety of control algorithms proposed for seismic vibration control, the idea of pseudo-negative stiffness (PNS) control, which aims to produce negative stiffness hysteretic loops, has been widely acclaimed because of its great advantages in practical application. Only the relative displacements and the relative velocities across control devices are required for measurement.

* Corresponding author

Iemura et al. [2], [3] first proposed the PNS control which can be realized taking advantage of semi-active control dampers, such as magneto-rheological (MR) dampers. The negative stiffness characteristic has also been observed in the study of the hysteretic loops of active control force produced by LQR algorithm [4], [5] and the effectiveness of negative stiffness on the damping efficiency was studied by Li [6] and Høgsberg [7]. There are generally four types of PNS control algorithms that have been proposed so far. The first one is the PNS viscous damping control algorithm, which shows a combination of a negative stiffness spring force term plus a viscous damping force term [2], [8], [9]. The maximum damping ratio of the PNS viscous damping control is demonstrated to be 53.4%. The second one is the PNS friction damping control algorithm, which generates a hysteresis curve similar that of the friction bearings plus the negative stiffness effect [10], [11]. The maximum damping ratio is demonstrated to be 64%, higher than the PNS viscous damping control algorithm. A simple displacement-based PNS control algorithm is also proposed to produce the PNS friction damping force by directly decaying the voltage of MR dampers linearly against the displacement [10], [12]. Since the control force at the original location remains almost constant, the simplified displacement-based PNS control algorithm is not expected to perform well for both low-to-moderate excitation level and extreme excitation level. Most recently, Wu proposed a PNS damping control algorithm which produce control forces with a triangular shape. The negative stiffness is only realized when the control device move towards its original location and the control force remains zero when the control device move away from its original location [13]. This control algorithm can achieve an effective performance but at the expense of requiring a large load capacity of control devices since it does not take full advantage of the energy dissipation capacity of semi-active dampers [14].

The control forces of the PNS control algorithms described above show a sudden change at velocity switches, which may cause structures experience a significant jerk especially under earthquakes rich of high-frequency component. In this study, a new filter-based PNS (FPNS) control algorithm is proposed to overcome this problem. By employing a low-pass filter, many other advantages are also obtained. Only displacement information is needed for feedback to compute the optimal active control force. A semi-active control design is developed to produce the FPNS force by MR dampers. Numerical analysis of the benchmark base isolated structure is presented to demonstrate the effectiveness of the proposed FPNS control algorithm by comparing the seismic responses with that of the sample semi-active control system, the simple displacement-based PNS control system and the passive viscous damping control system. Seismic records are scaled to different intensity levels to investigate the adaptability of each control system.

2 THE FILTER-BASED PSEUDO-NEGATIVE STIFFNESS CONTROL

A full semi-active control scheme is composed of two controllers. The primary controller is to calculate the desired reference control force using the structural output feedback and the specific control algorithm. The secondary controller is to calculate the control signal applied to the semi-active device to so as to generate the desired reference control force. The FPNS control algorithm is proposed to generate the desired reference control force and the MR dampers are employed to produce the control force acted on structures.

2.1 The filter-base PNS control algorithm

The load-displacement curve of the conventional PNS control force shows a sudden change at the times of velocity switch. This sudden change of control force may cause structures experience a significant jerk that is detrimental to structural performance. To address this problem, a simple filter-based PNS control algorithm is proposed to retain the characteristics of negative stiffness of control force while eliminating the demerit of the conventional PNS control force. The target control force can be given as

$$f_c(x_t)=\begin{cases} k_n x_t + f_0, & \text{if } x_t - x_{t-\Delta t} < 0 \\ k_n x_t - f_0, & \text{if } x_t - x_{t-\Delta t} \geq 0 \\ 0, & \text{if } f_c \times (x_t - x_{t-\Delta t}) < 0 \end{cases} \tag{1}$$

$$\dot{F}_c = -\zeta F_c + \zeta f_c \tag{2}$$

where k_n, f_0 and ζ are three control parameters defining the characteristics of the control force. $k_n < 0$ and denotes the negative stiffness. $f_0 > 0$ and denotes the friction force of f_c at the centre position. ζ is the filter parameter. x_t is the stroke of control devices at time instant t. f_c is an intermediate variable.

The behaviour of desired reference control force under harmonic excitations with different amplitudes (from 0.1 m to 0.5 m) and a period of 3 s are shown in Figure 1. It can be seen from Figure 1 that by employing a low-pass filter the control force changes smoothly at the velocity switches. Moreover, the control force at the original position increases with the increase of excitation intensity which is desirable to improve the structure functionality at low-to-moderate excitation intensity and improve the structure safety at extreme excitation intensity. In addition, the low-pass filter helps to roll off the control action at high frequencies where measurement noise and uncertainties may plague the controlled structure. Only the relative displacement across the control device is needed to produce the desired reference control force without the requirement of the feedback of the relative velocity across the control device, which is much difficult to obtain practically.

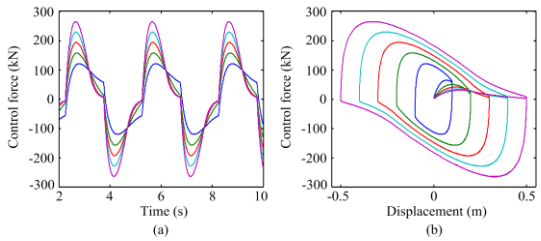

Figure 1. Time histories (a) and hysteresis loop (b) of the control forces with $k_n = 500$ kN/mm, $f_0 = 100$ kN and $\zeta = 5$ rad/s *under harmonic excitations with different amplitude and a period of 3 s.*

2.2 The semi-active control design using MR dampers

To induce the MR damper to approximately generate the desired reference control force, the command signal is selected as follows. When the MR damper force and the desired reference optimal force have different sign, the command voltage is set to zeros; otherwise, the instantaneous voltage applied to the MR damper is determined by assuming that the maximum voltage required to generate the maximum control force is 1 V, and for lower instantaneous control force, the voltage required is approximated by linearly relating it to the applied control force. The maximum control force of the MR dampers employed in this study is 2200 kN. The semi-active control design for selecting the command signal applied to MR dampers can be given as

$$v = V_c H(f_c f), \quad V_c = \begin{cases} \mu f_c, & V_c < 1 \\ 1, & V_c \geq 1 \end{cases} \tag{13}$$

where f_c denotes the desired reference control force based on the FPNS control algorithm; f denotes the control force produced by the control device; μ is the coefficient relating the control force to the voltage and equal to 1/2200 V/kN.

3 SEISMIC RESPONSE ANALYSIS OF THE FPNS CONTROL USING MR DAMPERS

3.1 Base isolated structure

The smart base-isolated benchmark building [15] is employed to investigate the performance of the FPNS controlled system. The number, location and the dynamic mechanical parameters of

the linear rubber bearings and MR dampers are the same as those described in reference [15]. The superstructure is assumed to be linear. The first three fundamental periods of the fixed base superstructure is 0.89 s, 0.78 s and 0.66 s. The fundamental periods of the base-isolated structure is 3 s and the inherent damping ratio of the isolation system is 3%. The computed model of the benchmark base-isolated building and the location of the bearing isolators and control devices are shown in Figure 1.

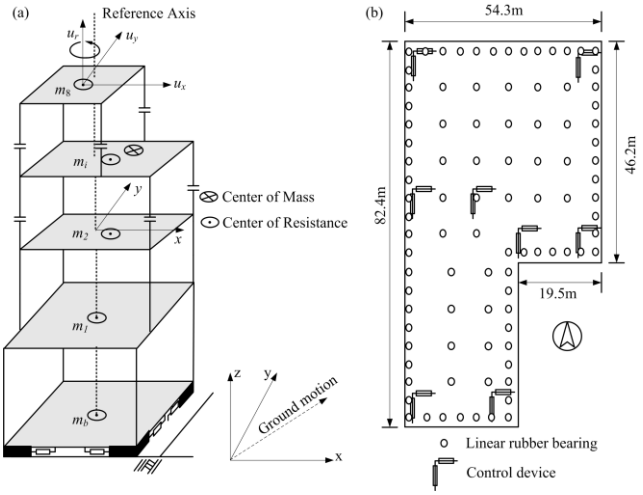

Figure 2. (a) Computed model of the benchmark base-isolated building; (b) the location of the bearing isolators and control devices.

3.2 Control systems

Four hybrid isolation systems are considered for comparison. In each case, the linear base isolation system is combined with a passive or a semi-active control system, which is installed in parallel with the linear isolation system. The considered control systems are FPNS control system, the simple displacement-based control system, the sample semi-active control system and the viscous damping control system. For the FPNS control system, the control parameters of k_n, f_0 and ζ for each MR damper are set to be -4230 kN/mm, 400 kN and 5 rad/s, respectively. As a result, the imposed negative stiffness is -0.4 times of the total bearing stiffness. The value of the control parameters chosen is demonstrated to be effective to improve the performance of the controlled system by conducting a series of parametric studies. For the simple displacement-based PNS control system and the sample semi-active control system, the control parameters are the same as those in reference [10] and [16], respectively. For the viscous damping control system, a parametric study is conducted to obtain the optimal damping ratio. The optimal damping ratio is defined to be the one that corresponds to the minimum base shear. The ratio of base shear to the total structural weight corresponding to different damping ratio from 0 to 95% is shown in Figure 3 for earthquake records of El Centro and Kobe. The optimal damping ratio are 40% for El Centro earthquake record and 30% for Kobe earthquake record. The average value of 35% is taken as the optimal damping ratio for the passive viscous control of the numerical analysis later on.

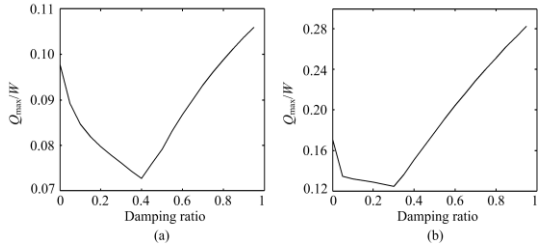

Figure 3. The ratio of base shear to the total structural weight corresponding to different damping ratio under El Centro earthquake record (a) and Kobe earthquake record (b) without scaling.

3.3 The ideal isolation control principal

The hybrid isolation control systems are commonly applied to critical facilities, such as hospital buildings and emergency units, which need to warrant operability during post-disaster emergency. This requires that an isolation control system can not only prevent structures from collapse but also prevent the disruption of structure functionality under extreme earthquake ground motions. On the other hand, with the rapid growth of social economy and improvement of living standard, the economic loss caused by the damage of non-structure components and contents becomes much higher than that caused by the damage of structure components. It indicates that, to reduce the economic loss, an isolation control system should also improve the structure functionality under low-to-moderate earthquake ground motions. To summarize, an ideal isolation control principle is to enhance the isolation safety for extreme earthquake excitations as well as improve the isolation functionality for low-to-moderate earthquake excitations and even extreme earthquake excitations if possible. The ideal isolation control principle can be used to evaluate the effectiveness of the proposed control scheme.

3.4 Simulation results

All control cases are analysed for earthquake records of El Centro and Kobe with the fault parallel (FP) and fault normal (FN) component acted in the building x-direction and y-direction respectively. The FN component is scaled to different intensity levels from 0 to 1 g and the same scaling factor is used for the FP component. The responses of base shear, base displacement (in both peak form and RMS form), inter-story drift ratio and floor acceleration (in both peak form and RMS form) are calculated for each case. The base displacement is related to the damage state of rubber bearing which is critical to isolation safety. The floor acceleration and the inter-story drift ratio are related to the damage state of interior contents and non-structure components respectively, which are critical to isolation functionality. Figure 4 shows the changes of responses under varying PGAs for each control system. Table 1 provides the maximum responses of base shear, base displacement, inter-story drift ratio and acceleration under intensity levels of 0.05 g, 0.2 g, 0.4 g and 0.8 g. The case of linear isolator alone is included to be used as a baseline to judge the effectiveness of other hybrid isolation control systems.

For the case of isolator alone, a good isolation efficiency (reduction in superstructure responses) can be obtained but at the expense of extensive base displacements at large seismic intensities which may threaten the isolation safety. Additional viscous damping can substantially reduce the base displacement, but the isolation efficiency decreases. For instance, the floor acceleration increases 29% and 133% for El Centro and Kobe respectively and the inter-story drift ratio increases 47% for Kobe when compared with the case of isolator alone. The benefit of the sample semi-active control is the significant reduction in base displacement but also at the cost of increased inter-story drift ratio and floor acceleration; however, the increases in the sample semi-active control are less than that of the viscous damping case for large seismic intensities. The advantage of the simple displacement-based PNS control is evident in significant reductions in the inter-story drift ratio and floor acceleration for large seismic intensities as compared to the sample semi-active control. For instance, the inter-story drift ratio and the floor acceleration decrease 8% and 28%, respectively, for El Centro earthquake record; and they decrease 23% and 37%, respectively, for Kobe earthquake record. However, significant increases in the superstructure responses (inter-story drift ratio and floor acceleration) are observed under low seismic intensities, which may cause much economic losses. The benefit of the FPNS control case is the reduction of superstructure responses under low seismic intensities as compared to the simple displacement-base PNS control. The superstructure responses are comparable to that of the isolator alone case for Kobe earthquake record and even further reduced for El Centro earthquake record. The base displacement for the FPNS control remains at the level of the simple displacement-based PNS control. Thus, it can be concluded that the FPNS control is effective in improving the isolation

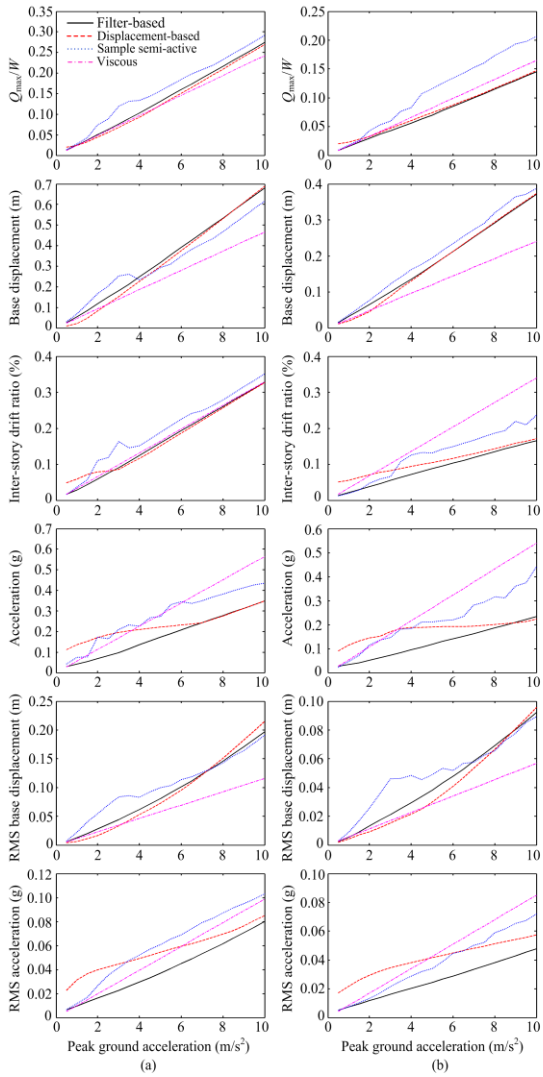

Figure 4. Comparison of responses under varying PGAs for earthquake records of El Centro (a) and Kobe (b). 'W' denotes the total structural weight.

functionality for low-to-moderate seismic excitations and even extreme excitations as well as enhance the isolation safety for high seismic excitations. In other words, the FPNS control system is the most optimal case to meet the requirement of the 'ideal isolation control principle'.

Figure 5 shows the change of control forces under varying PGAs for each control system. As expected, the control force increases with the increasing PGA for all the control case. The control force of the FPNS control is comparable to that of the simple displacement PNS control, slight lower than that of the semi-active control and substantially lower than that of the viscous damping control. It indicates the lower requirement of the capacity of control devices for the FPNS control system, which affects the cost of the project and practicality of control method.

Figure 6 presents the time-history curves and hysteresis curves of the control forces for the three hybrid semi-active control systems. For each case, the control force is produced by the MR damper at the centre of the base in x-direction. It is observed that the FPNS control force changes smoothly with the time and the displacement. Furthermore, the high frequency component of the control force is reduced. In addition, the FPNS control can limit its control force at low excitation level and shows a comparable energy dissipation capacity with that of the simple displacement-based FPNS control at lager excitation level. In contrast, the simple displacement-based PNS control system shows an almost fixed yielding force (force at the original position) for different seismic intensities. It is for these reasons that the FPNS control system can meet the 'ideal isolation control principle' well.

4 CONCLUSION

A filter-based PNS control algorithm is proposed. Only relative displacement information is required for feedback. By employing a low-pass filter, the control force shows a smooth change with the time and the displacement. The high frequency component is rolled off. Moreover, the FPNS control system produces a relative low control force at low excitation level, which limits the control force transmitted to the superstructure, while shows a large energy dissipation capacity at large excitation intensity.

A semi-active design is developed to produce the desired reference control force by MR dampers. The proposed FPNS control algorithm has been applied to the benchmark base-isolated structure. The responses are compared to that of the displacement-based PNS control case, the sample semi-active control case and the viscous damping control case. The results show that the displacement-based PNS control increases the superstructures responses significantly at low-to-moderate seismic intensities. In contrast, the superstructure responses of the FPNS control remain comparative or even lower than that of the linear isolator alone case for both low-to-moderate and high seismic intensities, while the base displacement is substantially reduced under extreme seismic excitations.

Table 1: Responses of each control case under seismic intensities of 0.05/0.2/0.4/0.8 g

Earthquake	Case of control	Base shear /structural weight	Base displacement (m)	Inter-story drift ratio (%)	Acceleration (g)
El Centro	Isolator alone	0.02/0.06/0.13/0.25	0.08/0.31/0.63/1.27	0.02/0.09/0.17/0.35	0.02/0.09/0.18/0.35
	FPNS	0.01/0.05/0.10/0.22	0.03/0.12/0.25/0.53	0.01/0.06/0.12/0.26	0.03/0.07/0.14/0.28
	Displacement-based	0.02/0.04/0.09/0.21	0.01/0.08/0.23/0.53	0.05/0.08/0.12/0.26	0.11/0.17/0.21/0.28
	Sample semi-active	0.01/0.07/0.13/0.23	0.03/0.17/0.23/0.47	0.02/0.11/0.15/0.28	0.04/0.17/0.23/0.38
	Viscous	0.01/0.05/0.10/0.19	0.02/0.09/0.19/0.37	0.02/0.07/0.13/0.26	0.03/0.11/0.23/0.45
Kobe	Isolator alone	0.01/0.04/0.08/0.17	0.04/0.15/0.31/0.62	0.01/0.05/0.09/0.19	0.01/0.05/0.09/0.19
	FPNS	0.01/0.03/0.06/0.12	0.01/0.07/0.14/0.29	0.01/0.04/0.07/0.14	0.03/0.05/0.10/0.19
	Displacement-based	0.02/0.03/0.06/0.12	0.01/0.04/0.13/0.29	0.05/0.07/0.09/0.14	0.09/0.14/0.19/0.20
	Sample semi-active	0.01/0.04/0.08/0.17	0.02/0.08/0.16/0.32	0.01/0.05/0.13/0.19	0.02/0.12/0.18/0.32
	Viscous	0.01/0.03/0.07/0.13	0.01/0.05/0.10/0.19	0.02/0.07/0.14/0.27	0.03/0.11/0.22/0.43

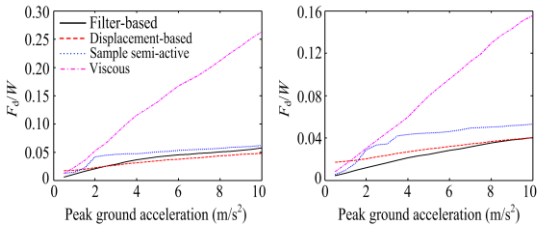

Figure 5. Comparison of control forces under varying PGAs for earthquake records of El Centro (a) and Kobe (b). 'W' denotes the total structural weight.

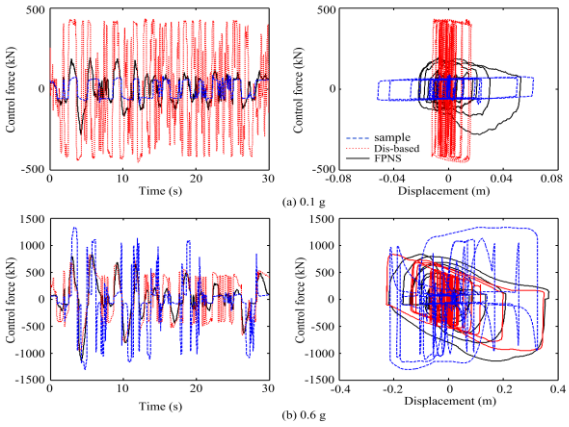

Figure 6. Control force varying with time and displacement for each control case under seismic intensities of 0.1 g and 0.6 g.

REFERENCES

[1] Kelly, J.M. The role of damping in seismic isolation. *Earthquake Engineering & Structural Dynamics* 1999; **28**:3-20.

[2] Iemura, H. & Pradono, M.H. Passive and semi-active seismic response control of a cable-stayed bridge. *Journal of Structural Control* 2002; **9**:189-204.

[3] Iemura H. & Pradono M. H. negative stiffness dampers for seismic retrofit of a cable-stayed bridge. *Proceedings of Passive Structural Control Symposium*, 2002: 7-16.

[4] Iemura H. & Pradono M.H. Simple algorithm for semi-active seismic response control of cable-stayed bridges. *Earthquake Engineering & Structural Dynamics* 2005; **34**:409-423.

[5] Li H., Liu M. & Ou J. Negative stiffness characteristics of active and semi-active control systems for stay cables. *Structural Control and Health Monitoring* 2008; **15**:120-142.

[6] Li H., Liu J. & Ou J. Seismic response control of a cable-stayed bridge using negative stiffness dampers. *Structural Control and Health Monitoring* 2011; **18**:265-288.

[7] Høgsberg J. The role of negative stiffness in semi-active control of magneto-rheological dampers. *Structural Control and Health Monitoring* 2011; **18**:289-304.

[8] Iemura H. & Pradono M.H. Application of pseudo-negative stiffness control to the benchmark cable-stayed bridge. *Journal of Structural Control* 2003; **10**:187-203.

[9] Madhekar S.N. & Jangid RS. Use of pseudo-negative stiffness dampers for reducing the seismic response of bridges: a benchmark study. *Bulletin of Earthquake Engineering* 2012; **10**:1561-1583.

[10] Iemura H., Igarashi A., Pradono M.H. & Kalantari A. Negative stiffness friction damping for seismically isolated structures. *Structural control and health monitoring* 2006; **13**:775-791.

[11] Iemura H., Igarashi A. & Kalantari A. Experimental verification and numerical studies of an autonomous semi-active seismic control strategy. *Structural Control and Health Monitoring* 2006; **13**:301-323.

[12] Pradono M.H., Iemura H., Igarashi A., Toyooka A. & Kalantari A. Passively controlled MR damper in the benchmark structural control problem for seismically excited highway bridge. *Structural Control and Health Monitoring* 2009; **16**:626-638.

[13] Wu B., Shi P. & Ou J. Seismic performance of structures incorporating magnetorheological dampers with pseudo-negative stiffness. *Structural Control and Health Monitoring* 2013; **20**:405-421.

[14] Gong W. & Xiong S. Probabilistic seismic risk assessment of modified pseudo-negative stiffness control of a base-isolated building. *Structure and Infrastructure Engineering*; 2015: 1-15.

[15] Narasimhan S., Nagarajaiah S., Johnson E. A. & Gavin H.P. Smart base-isolated benchmark building. Part I: problem definition. *Structural Control and Health Monitoring* 2006; **13**:573-588.

[16] Nagarajaiah, S., & Narasimhan, S. (2006). Smart base-isolated benchmark building. Part II: phase I sample controllers for linear isolation systems. *Structural Control and Health Monitoring*, ***13***:589-604.